# A quantum mechanical polarizable continuum model for the calculation of resonance Raman spectra in condensed phase

**ARTICLE** *in* THEORETICAL CHEMISTRY ACCOUNTS · MAY 2007

Impact Factor: 2.23 · DOI: 10.1007/s00214-006-0221-2



**4 AUTHORS:**

Benedetta Mennucci
Università di Pisa
**249** PUBLICATIONS **24,236** CITATIONS
SEE PROFILE

Chiara Cappelli
Scuola Normale Superiore di Pisa
**117** PUBLICATIONS **1,863** CITATIONS
SEE PROFILE

Roberto Cammi
Università degli studi di Parma
**152** PUBLICATIONS **16,223** CITATIONS
SEE PROFILE

Jacopo Tomasi
Università di Pisa
**347** PUBLICATIONS **40,294** CITATIONS
SEE PROFILE

Theor Chem Acc (2007) 117:1029–1039
DOI 10.1007/s00214-006-0221-2

REGULAR ARTICLE

# A quantum mechanical polarizable continuum model for the calculation of resonance Raman spectra in condensed phase

**Benedetta Mennucci · Chiara Cappelli · Roberto Cammi · Jacopo Tomasi**

Received: 14 July 2006 / Accepted: 13 October 2006 / Published online: 21 December 2006


**Abstract** In this paper we present two computational strategies to simulate resonance Raman spectra of solvated molecules within the framework of the polarizable continuum model (PCM). These two strategies refer to two different theoretical approaches to the RR spectra, namely the transform theory and the short-time dynamics. The first is based on the explicit detemination of the mimimum geometries of ground and electronically excited states, whereas the second only needs to know the Franck–Condon region of the excited state potential energy surface. In both strategies we have applied the recent advances achieved in the QM description of excited state properties and geometries of solvated molecules. In particular, linear response approaches such as CIS and TDDFT, and their extensions to analytical gradients, are here used to evaluate the quantities required to simulate resonance Raman spectra. The methods have been applied to the study of solvent effects on RRS of julolidine malononitrile (JM). The good agreement found between the calculated and experimental RR spectra seems to confirm the reliability of the computational strategies based on the PCM description.

## 1 Introduction

Raman scattering is the result of the coupling between the radiation and the components of the molecular polarizability which are modulated by molecular vibration. In Raman scattering measurements where the wavelength of the radiation is close to an electronic excitation of the molecule, the intensity of the signal can be enhanced by a factor of up to $10^4$–$10^6$. This process is referred to as resonance Raman scattering (RRS) [1].

One of the main interests in RRS is that this spectroscopic technique yields information about electronically excited state properties and structure. There are in fact very few experimental measurements from which one can obtain excited state data, by contrast there have been important recent advances in QM theories to describe excited state geometries and properties. It thus becomes very useful to compare the results obtained with such new techniques with those extracted from RRS.

Along this line, theoretical and computational approaches have to become more and more realistic so to include all the most important effects which can determine the nature and the properties of the various electronically excited states. Among these effects, a very important role is obviously played by the solvent. It is in fact well known that polar solvents can largely affect the electronic nature of excited states, for example amplifying their charge-transfer character. These strong electronic deformations in the solvated molecules are obviously accompanied by structural deformations which can lead to very different relaxed excited states with respect to the same systems in gas-phase. For all these reasons it is of large interest to develop QM models which can determine properties and structures of molecular excited states taking into account the possible effects of the solvent. Among the available approaches, one of the most suited to be applied to this kind of study is represented by continuum solvation

B. Mennucci (✉) · C. Cappelli · J. Tomasi
Dipartimento di Chimica, Università di Pisa,
via Risorgimento 35, 56126 Pisa, Italy
e-mail: bene@dcci.unipi.it

R. Cammi
Dipartimento di Chimica, Università di Parma,
Viale delle Scienze 17/A, 43100 Parma, Italy

models. These latter in fact can be (and they have been) extended to almost all the main QM description used to describe excited states. In particular, the polarizable continuum model (PCM) developed in Pisa by Tomasi et al. [2–5] has shown to give reliable descriptions of different phenomena involving electronically excited states.

The extension of QM continuum models to excited states has been discussed in various papers (see, e.g. reviews such as [6,7] for an extended literature). The main specificity is related to the fact that the electronic excitation is a process involving not only the solute but the entire solute–solvent system. As a consequence, the definition of the excited states of molecular solutes requires also the characterization of the solvent degrees of freedom. The difference of the characteristic time scale of the electronic degrees of freedom of the solute and the composite degrees of freedom of the solvent may lead to different excited state regimes, with two extreme situations, namely the "nonequilibrium regime" in which the slow degrees of freedom of the solvent are not equilibrated with the excited state electronic redistribution upon vertical excitation processes, and the "equilibrium regime" in which the solvent is allowed to equilibrate i.e., reorganizes all its degrees of freedom including the slow ones. In polar solvent, the different regimes may largely influence the properties of the solute excited states, and thus computational algorithm should allow for the use of both of them.

Recently, a further important specificity of the extension of QM continuum models to describe excited states has been rigorously analyzed both from a formal and a numerical point of view [8,9]. In such an analysis, it has been shown that the application of these models to either linear response (random phase approximation, RPA, configuration interaction-singles CIS, and time-dependent density functional theory,TDDFT) or state specific approaches (complete active space self-consisting field, CASSCF, configuration interaction CI, etc.) may lead to differences due to an intrinsic nonlinear character of the solvent response operators used in continuum models. The state specific (SS) approaches, which are based on the explicit calculation of the excited state wave function, properly take into account the variation of the solute–solvent interaction accompanying the change of the electronic density during an electronic excitation, while the linear response methods introduce only effects related to the corresponding transition density. In order to reduce these intrinsic differences, recently we have presented a method in which a SS correction is introduced in LR approaches [10]. This method is based on the use of the relaxed density which can be obtained in LR approaches thanks to their extension to analytical gradients now available not only within the CIS version but also within TDDFT. In the present paper, these two techniques and their gradient extensions [11,12] will be applied to model RRS of solvated systems.

In particular, two different theoretical approaches will be presented to describe RRS. The first is the transform theory (TT) approach by Peticolas and Rush [13] which allows the calculation of relative resonance Raman intensities from Franck–Condon (FC) type scattering based on the optical absorption spectrum of a particular compound and the differences in the equilibrium structures between the ground and the excited state in resonance. The second, alternative, approach is based on the formalism developed by Lee et al. [14,15] by recasting the original Kramers, Heisenberg, and Dirac (KHD) formalism [16,17], into a time-dependent formalism in terms of wave-packet dynamics.

After a short introduction into the RRS theories in Sect. 2 to clearly describe the specificities introduced in both TT and STD by the presence of the solvent, results are presented for julolidine malononitrile in Sect. 3. We will focus on density-functional theory (DFT) methods for the calculation of excited-state energies and structures, in comparison to the Hartree–Fock (HF)/CIS approach. A discussion of the results and a conclusion are given in Sect. 4.

## 2 Theory for resonance Raman in solvated systems

In this section we first review the fundamental aspects of TT and STD approaches and then we describe which specific aspects are involved when a PCM solvent is introduced.

### 2.1 Transform theory

The transform theory of resonance Raman intensities is based on the optical theorem, which connects the optical absorption with the imaginary part of the polarizability tensor components, and on the Kramers–Kronig relations between the real and the imaginary part of the polarizability tensor components.

Five are the "standard assumptions" made in the TT approach [13]: (1) the Born–Oppenheimer approximation is valid, (2) only one excited electronic state is important (from now on indicated with $r$), (3) ground- and excited-state potential energy surfaces are harmonic, (4) non-Condon effects are negligible, i.e., only FC-type scattering is important, (5) excited and ground-state normal coordinates differ only in their equilibrium

positions, so that Duschinsky rotations are not important and the frequencies for ground and excited-state vibrations are the same ("independent mode, displaced harmonic oscillator model", IMDHO [18])

Within these approximations, the vibrational Raman-scattering cross section from an initial vibrational state i to a final state f of the electronic ground state is proportional to the square of the polarizability tensor whose component $\rho\sigma$ is given by

$$\alpha^{fi}_{\rho\sigma}(\omega_0) = \frac{M^e_{0r,\rho} M^e_{0r,\sigma}}{\hbar} \sum_k \frac{\langle \nu_f | \nu_k \rangle \langle \nu_i | \nu_k \rangle}{\omega_{ki} - \omega_0 - i\Gamma_r} \tag{1}$$

where the damping constant $\Gamma_r$ is the total homogeneous linewidth (halfwidth at half-maximum) from both pure dephasing and lifetime contributions, $\omega_0$ denotes the laser excitation frequency and

$$\omega_{ki} = \omega_{r0} + \sum_{j=1}^{3N-6} \nu_j \Omega_j$$

where $\Omega_j$ is the harmonic vibrational frequency corresponding to normal mode j, $\hbar\omega_{r0}$ is the energy difference between the $v = 0$ levels of the electronic ground and excited state $r$.

In Eq. (1) the summation over intermediate states has been restricted to vibrational levels of a single resonant electronic state (the state $r$), and the Condon approximation has been imposed such that the dipole moment matrix elements have been separated into products of a purely electronic transition moment ($M^e_{0r}$) and a vibrational overlap.

One important point in the transform-theory approach is that, for the "independent mode, displaced harmonic oscillator model," the FC-type integrals are known analytically in terms of the normal-mode dimensionless displacements $\Delta_j$ of the excited state equilibrium structure. As a result, the relative RRS intensities can be approximated as

$$i_j^{1\leftarrow 0} / i_k^{1\leftarrow 0} \simeq \Delta_j^2 / \Delta_k^2 \tag{2}$$

where we have neglected the frequency-dependent prefactor which may be taken to be constant in a good approximation [19]. We note that these normal coordinate displacements correspond to dimensionless normal coordinates $q_j$, and thus

$$\Delta_j = \sum_k^{3N-6} L^{-1}_{jk} \Delta R_k \tag{3}$$

where $L^{-1}_{jk}$ are the elements of the **L** inverse matrix determined from the solution of the ground state normal-mode eigenvalue problem [20], and $\Delta R_k$ are the changes in the internal coordinates upon excitation of the molecule into the relevant excited state.

The expression (2) states that relative RRS intensities are completely determined once ground and excited state minimum geometries are known together with the ground state vibrational normal modes.

### 2.2 TD theory: the short time dynamics approximation

An alternative, time-dependent formalism for the calculation of resonance Raman intensities has been developed by Lee et al. [14,15] by recasting the original formalism developed by Kramers, Heisenberg, and Dirac into a time-dependent formalism in terms of nuclei wave-packet dynamics. Although this time-dependent formulation is similar to the transform theory, it differs in the interpretation of Raman scattering in terms of wave packets and the semiclassical propagation of them. This approach showed that many features of both resonant and nonresonant Raman scattering could be understood in terms of short-time dynamics.

Within the time-dependent theory, the polarizability tensor becomes

$$\alpha_{\rho\sigma} = \frac{M^e_{0r,\rho} M^e_{0r,\sigma}}{\hbar} \int_0^\infty \mathrm{d}t \, \langle f \, | i(t) \rangle \exp\left[ i \left( \omega_L + \omega_i - \omega_{r0} \right) t - g(t) \right] \tag{4}$$

where $\omega_i$ is the vibrational frequency (above the zero point) of the $|i\rangle$ vibrational level of the ground electronic state, and

$$|i(t)\rangle = \exp\left(-iH_{\mathrm{vib}} t/\hbar\right) |i\rangle \tag{5}$$

$H_{\mathrm{vib}}$ being the Hamiltonian for vibrational motion in excited state. The quantity $\langle f \, | i(t) \rangle$ is a time-dependent vibrational overlap between the final vibrational state and the initial state propagated for time $t$ by the excited state vibrational Hamiltonian and $g(t)$ is a lineshape function. It is interesting to note that in this time-domain formulation, contrary to the frequency dependent expression, it is much easier to incorporate possible solvent effects in the dephasing. This can be obtained for example introducing a Brownian oscillator approach and thus at the end the lineshape function $g(t)$ will incorporate both lifetime decay and solvent-induced pure dephasing [21].

The time dependence of $|i(t)\rangle$ represents the motion of the nuclei after the potential energy function is instantaneously (on the time scale of vibrational motion) switched from that of the ground electronic state to that of the excited state. The intensity of each Raman transition depends on the overlap of $|i(t)\rangle$ with a different final state. In general, those modes that undergo the largest

excited-state geometry changes will exhibit the highest intensities. In polyatomic molecules, each overlap $\langle f\ |i(t)\rangle$ involves all vibrational coordinates.

Equation (4) implies that the time scale of the dynamics that contributes to the resonance Raman intensity should extend for as long as the damping factor is non-negligible. In practice, though, in most fairly large molecules the intensities are determined almost entirely by the dynamics within less than a vibrational period (typically only 10–20 fs or so). In this "short-time dynamics" (STD) limit, the relative RRS intensities can be approximated as

$$i_j^{1\leftarrow 0}/i_k^{1\leftarrow 0} = \left(\frac{\partial E_{\mathrm{el}}^x}{\partial q_j}\right)^2 \Big/ \left(\frac{\partial E_{\mathrm{el}}^x}{\partial q_k}\right)^2 \tag{6}$$

where $E_{\mathrm{el}}^x$ is the electronic excitation energy, $q_j$ and $q_k$ are the normal coordinates of modes $j$ and $k$, respectively and the derivatives are computed at the ground-state equilibrium position. This equation means that when only short-time dynamics is important the relative intensities are given by the gradient of the Franck–Condon vertical excited-state surface with respect to the normal coordinates. In this case, no explicit knowledge of the excited state minimum structure is required.

Such an expression can be related by the TT expression (2) by defining the partial derivative of the excited-state electronic energy with respect to a ground-state normal mode at the ground-state equilibrium position in the IMDHO model [1],

$$\left(\frac{\partial E_{\mathrm{el}}^x}{\partial q_j}\right)_{\mathrm{gs}} = -\Omega_j \Delta_j \tag{7}$$

TT and STD methods combined can be used to check the internal consistency of the approximations made with respect to the excited-state potential energy surface [22].

### 2.3 PCM for TT and STD descriptions

In the previous sections we have reviewed the theoretical expressions for the resonance Raman intensities in the TT and STD approaches when a single excited electronic state contributes to the optical response. These expressions when applied to solvated systems should include, in principle, the changes in nuclear equilibrium geometry (reorganization) along all solute vibrational modes plus a collective solvation coordinate, and also allow for the possibility of inhomogeneous broadening of the electronic transition and broadening due to the finite lifetime of the excited electronic state.

In the present study, however, the aspect of the broadening of the RR band will not be considered and thus the analysis of the solvent effects will be applied to the final approximate expressions of the TT and STD theories (Eqs. (2) and (6), respectively). In doing this, we certainly cannot account for the presence of the solvent on the bandshape but we include solvent effects on the position and the shape of the ground and electronic state potential energy surfaces. These effects are surely the dominant ones for a proper description of the RRS of solvated systems, especially when these latter are (like in the present paper) conjugated push–pull systems in which the fractional charge-transfer character, or degree of bond-order alternation, is tunable by changing the polarity of the solvent.

The main effects of the solvent on RR spectra (position of the peaks and their intensities) can thus be ascribed to two different origins: one due to the solvent-induced changes in the geometry of both ground and excited states and the other due to the variations induced in the electronic distribution of both states.

In order to take into account these two effects, the QM description of the solute has to account for the solvent at each step, namely the determination of the ground state minimum geometry and of the corresponding vibrational normal modes and frequencies, and the determination of the vertical excited state (in the STD scheme) or the relaxed excited state (in the TT scheme).

As far as concerns ground state geometry and vibrational modes and frequencies, PCM has been already successfully applied to describe IR [23] and normal Raman [24] spectra of solvated systems. Here, we thus do not repeat what already presented in those studies but we just recall that the interested reader can find all the details of the implementation of the PCM theory within those spectroscopies in the cited paper or in recent reviews such as [6,25].

It is instead of interest to focus on the modelization of the PCM solvent effects on excited states. The application of PCM to TT and STD theories in fact involves the determination of portions of the PES for the solvated excited state.

As briefly discussed in Sect. 1, the new specific aspect introduced in the modelization of excited state formation and relaxation in solution is the dynamics of the solvent. In particular, in fast processes, such as electronic excitations, electron transfers or ionizations, the time-scale of the change in the charge density of the solute is usually much smaller than the time-scale in which a polar solvent fully relaxes to reach a new equilibrium state. During this relaxation, the solvent nuclear and molecular motions act as inertia on the solvation response and a nonequilibrium regime is established. Due to the mutual solute–solvent polarization, the new equilibrium is reached through changes of both solute and solvent, and an accurate description of the reorganization path

should consider the evolution of their interaction and, possibly, the solute geometry relaxation.

If now apply this analysis to the TT and STD schemes we obtain that, when relaxed excited states are considered as in TT, a solvation equilibrated to the relaxed state should be used while, when a FC portion of the PES has to be explored as in STD, nonequilibrium solvation is to be preferred. In this latter case, a partition of the PCM effect in two separate components is done, one related to the dynamic (or fast) electronic response of the solvent, and the other to the slower, or inertial, response connected to nuclear and/or molecular motions inside the solvent [26–28]. According to what was said before, the dynamic component will depend on the instantaneous charge distribution of the solute and on the optical dielectric constant. The inertial component, on the contrary, will still depend on the solute charge distribution of the initial (ground) state.

The theory of the extension of PCM to excited states and their derivative approaches has been already presented both at CIS [11] and TDDFT level [12] and successfully applied to different organic molecules. Here, we only recall that for both methods, the energy functional to differentiate is the free energy $G$ defined as

$$G = E - \frac{1}{2}\left\langle \Psi \left| V^{\mathrm{PCM}} \right| \Psi \right\rangle \tag{8}$$

where $E$ is the eigenvalue of the effective Hamiltonian $(H^0 + V^{\mathrm{PCM}})$ including the PCM operator $V^{\mathrm{PCM}}$. This solvent induced term represents the electrostatic interaction between the solvent and the solute's nuclei and electrons. In the computational practice a boundary-element method BEM is applied by partitioning the cavity surface into discrete elements, called tesserae, and by representing the solvent response with a collection of apparent point charges, each one placed at the center of a tessera. The detailed expression of the linear system of equations defining such charges depends on the specific version of the PCM method being used and it has been previously published (see Ref. [6] for a complete survey). Here we simply recall that such equations are determined by the form and shape of the cavity, by the details of the discretization of the surface and by the solvent permittivity $\epsilon$. By tuning the value of $\epsilon$ we can describe the changes in the solvation of the excited state when passing from the Franck–Condon region of the solvent coordinate i.e., the nonequilibrium to a completely relaxed solvent. This is done by changing the value of $\epsilon$ used to compute the PCM charges from the optical value $\epsilon_\infty$ namely, the square of the refractive index to the static bulk value $\epsilon_0$. Effects of these changes can be significant for polar solvent for which $\epsilon_\infty \ll \epsilon_0$.

The QM treatment of the PCM operator $V^{\mathrm{PCM}}$ is delicate, as it depends on the solute total density and thus it induces a nonlinear character in the solute Schrödinger equation. This nonlinearity for ground electronic states is automatically solved by using standard self-consistent field iterative approaches developed for isolated systems. Passing to excited states, instead, two different solvent-specific approaches have been developed: (i) a general scheme in which the excited state problem described using state specific (SS) approaches (complete active space self-consisting field CASSCF , CI, etc.) is iteratively solved in the presence of the corresponding solvent response and (ii) a simplified scheme in which, following a linear response (LR) formalism, the solvent response is determined by transition densities instead of state densities. Recently, we have shown the intrinsic differences between the two schemes [8,9] and we have formulated a third hybrid scheme in which the computationally efficiency of LR approaches is combined to the more satisfactory description of the solvent response of SS approaches [10]. This third scheme (also indicated as corrected LR, cLR) introduces a SS correction in the original LR description using the PCM charges produced by the relaxed density of each excited state which can be obtained in LR approaches thanks to their extension to analytical gradients. This corrected LR approach reduces the differences with respect to a real SS scheme and it allows for a more satisfactory description of the variation of the solute–solvent interaction accompanying the change of the electronic density during an electronic excitation.

In the following application to the simulation of RR spectra of a solvated push–pull molecule we will use both an equilibrium PCM-TT and a nonequilibrium PCM-STD description. In the latter case, both the standard LR and the corrected LR method will be tested.

## 3 Resonance Raman of julolidine malononitrile

In this section we report the application of the methodologies for the study of RRS in solution reported in the previous section to the evaluation of a relevant portion of the resonance Raman (RR) spectrum of julolidine malononitrile (JM) in solvents of different polarity. The experimental investigation of solvent effects on RR spectra of JM has been reported previously in Refs. [29,30].

JM belongs to the class of conjugated organic molecules of interest for second-order nonlinear optical applications, due to the fact that it has reported to have low-lying electronic transitions with a high degree of intramolecular charge-transfer (CT) character and

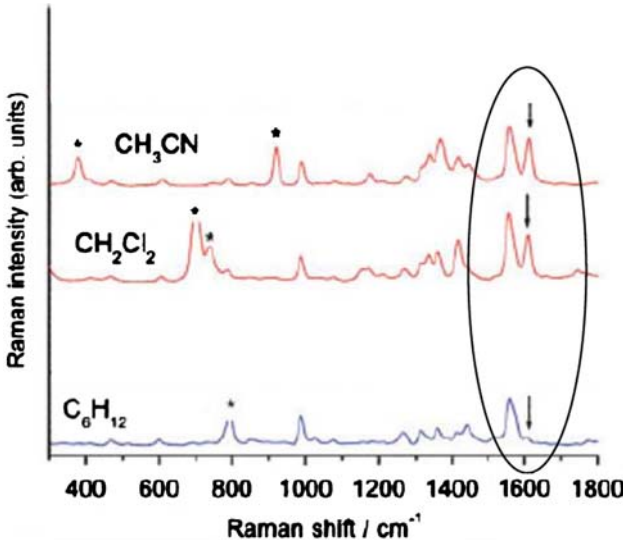


**Fig. 1** Resonance Raman spectra of JM in different solvents after subtraction of fluorescence backgrounds. *Asterisks* label solvent bands. *Arrows* mark a vibration whose intensity is particularly solvent dependent. The spectra are taken from Ref. [30]

consequently is sensitive to changes in the local solvent environment.

As it has been reported previously in the literature [29,30] experimental RR spectra of JM exhibit a marked dependence upon the solvation environment (see Fig. 1).

In the experimental RR spectrum, the most strongly solvent-dependent vibration seems to be that at 1612 $cm^{-1}$. Such a vibration involves the stretching of the bonds defining the phenyl, which are aromatic in the neutral form but can be considered double bonds in the zwitterionic form. A strong resonance Raman intensity is experimentally evidenced for this band, suggesting large geometry change in this mode upon electronic excitation.

In the following we shall test the predictive power of PCM in reproducing the intensity pattern of the RR lines in the range 1550–1620 $cm^{-1}$ by exploiting the two different methodologies described in the previous section and assuming that CT lowest energy strongly allowed transition is the only state determining the RR spectrum [31].

### 3.1 Computational details

The calculations of ground state energies, geometries, vibrational frequencies and normal modes were performed by exploiting Hartree–Fock (HF) and density functional theory (DFT) with the B3LYP hybrid functional. The basis set chosen was 6-311G(d,p), e.g. the same used in the previous study by Myers et al. [29,30].

For the calculation of excited states CIS and TDDFT (using the same basis set) were applied to the calculation of excitation energies and geometries. Solvent effects were accounted for by exploiting the integral equation formalism (IEF) [4,5] version of the PCM as implemented in a development version of the Gaussian code [32].

Calculations of excitation energies were performed by using both the linear response (LR) and the "corrected LR" schemes (see Sect. 2.3). In all the calculations in solution, a molecule-shaped cavity was used, made of interlocking spheres centered on heavy atoms and using for the radii of the spheres the default values implemented in Gaussian.

### 3.2 Ground and excited state geometries

Before presenting results about the RRS intensities we analyze ground and CT excited state geometries.

The variation in selected bond lengths (see Fig. 2 for their labeling) for JM ground state passing from cyclohexane to acetonitrile is reported in Fig. 3, where HF and DFT/B3LYP are compared.

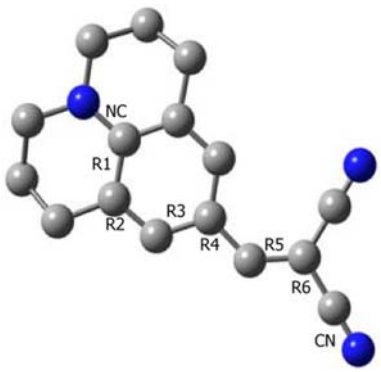


**Fig. 2** Scheme of JM structure with labelling of selected distances

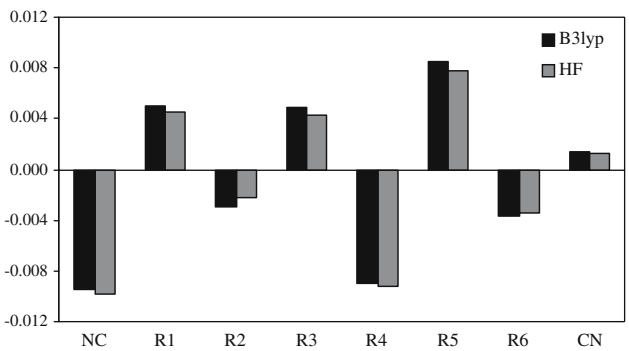


**Fig. 3** Variation in selected bond lenghts (see Fig. 1) of JM ground state passing from cyclohexane to acetonitrile. HF and DFT/B3LYP results are compared

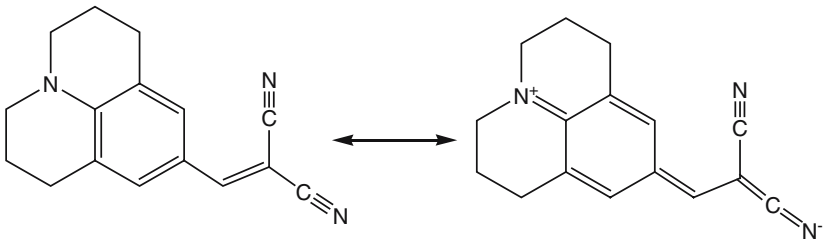

**Fig. 4** Pictorial representation of the neutral and the zwitterionic resonance forms for JM

**Table 1** B3lyp/6-311G(d,p) vibrational frequencies ($cm^{-1}$)

| | Gas | $C_6H_{12}$ | $CH_2Cl_2$ | $CH_3CN$ |
|---|---|---|---|---|
| M1 | 1589 | 1585 | 1581 | 1580 |
| M2 | 1604 | 1595 | 1586 | 1584 |
| M3 | 1651 | 1650 | 1648 | 1647 |

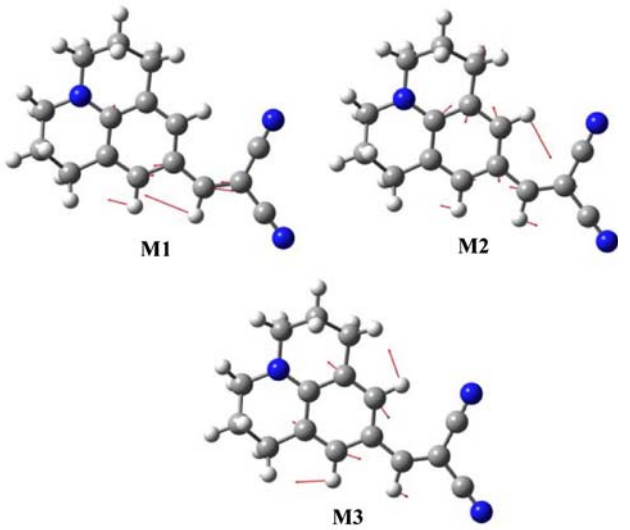


**Fig. 5** Cartoon of normal modes corresponding to M1, M2 and M3 vibrations of JM based on B3LYP/6-311G(d,p) calculations

The solvent dependence of the ground state coordinate changes reported in Fig. 3 are qualitatively consistent with a two-state model, pictorially represented in Fig. 4.

More specifically, as solvent polarity increases, the ground state displays a more zwitterion-like structure: with increasing solvent polarity and increasing zwitterionic character, we observe an alternate positive and negative variations of the single and of the double bond lengths along the whole skeleton going from the amino to the cyano nitrogen. The expected solvent dependence of the conjugated bond lengths is easily deduced by inspection of the resonance forms in Fig. 4. This behavior is almost identical both at the HF and DFT level of description. Due to this equivalence, in the following we shall limit the ground state description to the DFT level.

In Table 1 we report the DFT/B3LYP vibrational frequencies of the modes corresponding to the region of the RR spectrum showing the largest solvent effects (see Fig. 1) and in Fig. 5 a pictorial view of the corresponding normal modes.

The solvent effects on frequencies are not large. This is especially true for the mode labelled as "mode 3 (M3)" which corresponds to a "quinoidal" stretch of the julolidine ring (stretching of the phenyl bonds). Such an insensitivity is confirmed by experimental RRS spectra. More pronounced solvent effects are found for the other two modes (M1 and M2) for which differences of the order of 10 and 20 $cm^{-1}$, respectively, are calculated passing from gas phase to the most polar solvent. These differences well correlate with the differences found in the bond lengths; for example, M2 mode for which the largest solvent shift is obtained, can be characterized by a stretching of the R4 bond for which in Fig. 3 we found the largest solvent sensitivity (together with NC).

Moving to the CT excited state geometry, the results largely depend on the QM level of calculations.

In Fig. 6 we report the ground-to-excited state variations in the single and double bond of the JM skeleton as obtained at CIS or TDDFT level. Note that all the values reported in figure are obtained in both cases by considering the DFT ground state; however, almost identical results are found by considering the HF ground state. At TDDFT level we could not locate the excited state minimum for the isolated system.

The inspection of Fig. 6 clearly reveals a deficiency of TDDFT in describing ground-to-excited state structural changes in JM. In fact, if we adopt the two-state picture used to explain solvent effects on ground state geometry, also here we should expect the typical alternation of positive and negative variations in single and double bonds which indicate an enhanced zwitterionic character in the excited state. This alternation is correctly reproduce by CIS but not by TDDFT. These findings are not unexpected, as TDDFT, at least with the hybrid B3LYP functional, has been reported to be unsuitable for the description of charge-transfer conjugate systems

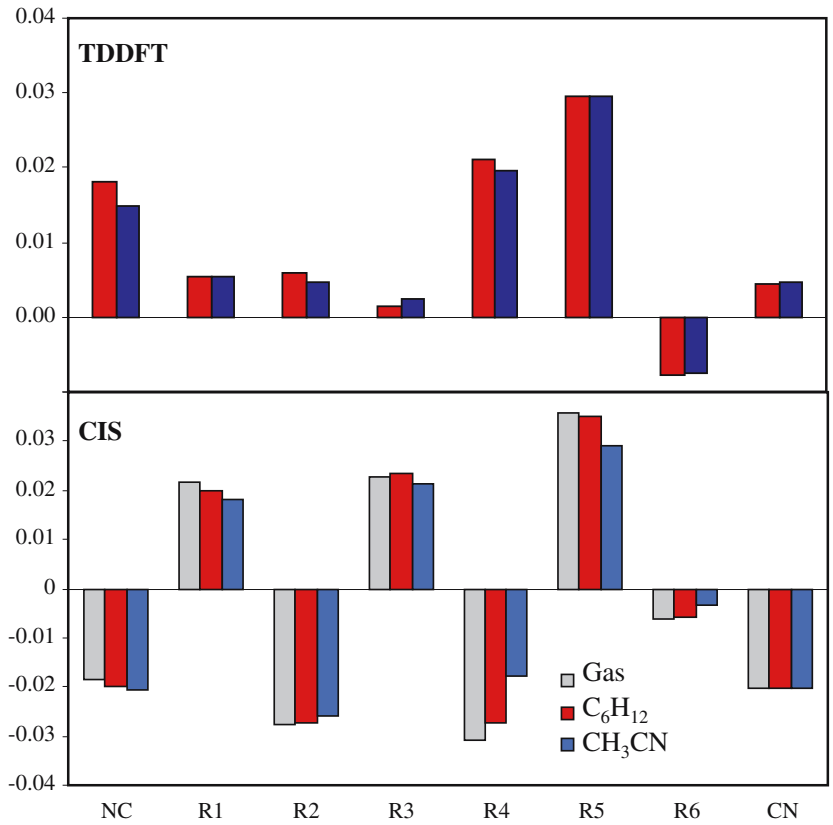


**Fig. 6** Variation in selected bond lenghts (see Fig. 2) of JM from ground to excited state in gas, cyclohexane and acetonitrile. Both CIS and TDDFT/B3LYP are reported

[33–35]. For this reason, in the following we will resort only to CIS for the evaluation of RRS spectra.

### 3.3 Excited state displacements and RR intensities

In this section we report the results obtained for the adimensional ground-to-excited state displacements, $\Delta_j$, using the two different methodologies presented in Sect. 2, i.e. TT which gives directly the displacements by considering ground and excited state geometries and ground state normal modes, and STD-IMDHO, where instead a $\Delta_j$ value is indirectly obtained in terms of the gradient of the excitation energy in the FC region, i.e. no information on the excited state minimum geometry is required (see Eq. (7)).

The results obtained with the two theories are reported in Tables 2 and 3, respectively. In the case of TT the displacements have been calculated by using Eq. (3) and taking care that both ground and excited states have the same center of mass and their structures are oriented so to have coincidence in the principal axes of inertia. In the case of STD, for the evaluation of the excited state gradients we have tested both the LR and the corrected LR approximations (see Sect. 2.3 for more details).

The two alternative approaches, TT and STD (either in the LR or cLR version) give qualitatively similar results, although they resort to different approximations and involve completely different assumptions on the solvation regime (equilibrium vs. nonequilibrium, see

**Table 2** Adimensional ground-to-excited state displacements, $\Delta_j$, obtained with the TT method at CIS level (using the DFT ground state geometry) for the M1, M2 and M3 normal modes

| | Gas | $C_6H_{12}$ | $CH_2Cl_2$ | $CH_3CN$ |
|---|---|---|---|---|
| M1 | 0.388 | 0.345 | 0.248 | 0.197 |
| M2 | −0.523 | −0.405 | −0.201 | −0.142 |
| M3 | 0.249 | 0.263 | 0.267 | 0.249 |

**Table 3** Adimensional ground-to-excited state displacements, $\Delta_j$ obtained with the STD method at CIS level (using the DFT ground state geometry)

| | Gas | $C_6H_12$ | $CH_2Cl_2$ | $CH_3CN$ |
|---|---|---|---|---|
| | | LR | | |
| M1 | 0.412 | 0.397 | 0.302 | 0.252 |
| M2 | −0.538 | −0.477 | −0.243 | −0.175 |
| M3 | 0.444 | 0.470 | 0.413 | 0.392 |
| | | cLR | | |
| M1 | – | 0.318 | 0.220 | 0.187 |
| M2 | – | −0.335 | −0.139 | −0.098 |
| M3 | – | 0.394 | 0.332 | 0.323 |

For solvated systems both the LR and the corrected LR approximations are presented

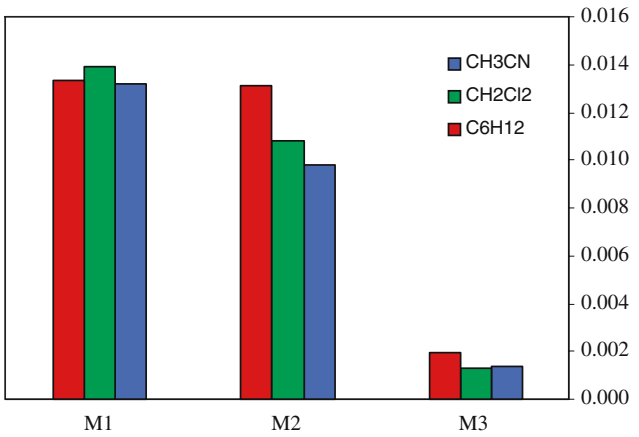


**Fig. 7** Variations in the dipole moment of the excited state (in debye) with respect to the three selected normal modes

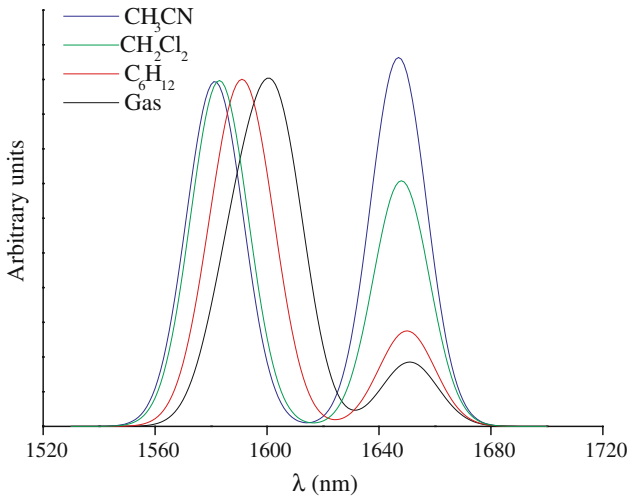


**Fig. 8** TT resonance Raman intensities in gas and in various solvents. All spectra have been scaled to have approximately equal intensities in the band near 1580 $cm^{-1}$

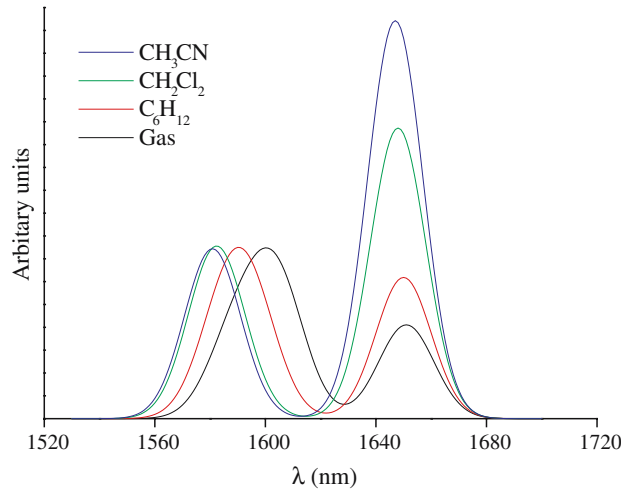


**Fig. 9** STD (cLR) resonance raman intensities in gas and in various solvents. All spectra have been scaled to have approximately equal intensities in the band near 1580 $cm^{-1}$

Sect. 2.3). In both cases, a decrease of the displacement passing from the isolated to the solvated system is observed for all the modes, being the largest changes found for M2. Such a behavior is in line with what already pointed out for frequencies (see Table 1).

To support these structural data with related electronic properties, in Fig. 7 we report the value of the variation of the excited state dipole moment with respect to the selected normal coordinates (we recall here that our approach relies on the assumption that frequencies, and normal coordinates, are the same for the ground and the excited state).

The observed trends in changing the solvent well correlate with what found for the adimensional ground-to-excited state displacements, $\Delta_j$: low variations (and low solvent sensitivity) along the M3 mode and larger variations for the other two modes with M2 presenting the largest solvent sensitivity.

If we now compare the results obtained for both displacements and variations of dipole moments with experimental RR spectra (see Fig. 1), it might be concluded that an opposite behavior is found for M3 for which experiments seems to show a large sensitivity to the solvent while very low sensitivity is found with PCM calculations. As a matter of fact, the disagreement between calculations and experiments is only apparent for the reasons which follow.

In Figs. 8 and 9 simulated RRS spectra obtained by transforming TT or STD(cLR) displacements into RRS intensities are shown. Such intensities were obtained by using the approximated formula (2) and (6) and by simulating the spectrum with lorentzian band shapes. In addition a scaling of the spectra was introduced, exactly as done in the experiments [29]: this scaling is done so to have approximately equal intensities of the strong line (corresponding to a combination of M1 and M2) in all the solvents.

As it can be seen, the band corresponding to M3 is now largely sensitive to the solvent and it correctly increases passing from gas to solution, and from apolar to polar solvent, exactly as found in the measured RRS spectra. Both TT and STD approaches are able to reproduce the experimental trend, although the relative intensities of the two bands are not quantitatively reproduced for the more polar solvents, where an overestimation of the intensity of the M3 band is observed. From this analysis based on calculated RR spectra, it thus follows that the experimentally observed sensitivity of the M3 band with the solvent is indeed a kind of an

artifact induced by the other two adjacent bands which both significantly decrease passing from gas-phase (or apolar solvent) to polar solvents.

## 4 Conclusions

In this paper we have presented two computational strategies to simulate resonance Raman spectra of solvated molecules based on the transform theory and short-time dynamics theory. In both strategies important approximations have been used, however the results obtained for the test case seem to confirm their reliability, at least to get the correct qualitative picture of the solvent effects on the position and the intensity of the RR bands. These results have surely to be confirmed on other systems before they can represent a stated proof of the validity and the accuracy of the theoretical methods and of the computational strategies. The main important goal of this study, however, was not the definition of a theory for resonance Raman scattering in solution which covers all the aspects of the solvent effects, but instead an attempt to exploit the recent advances achieved in the QM description of excited state properties and geometries of solvated molecules. In particular, the recent implementation of analytical gradients for time-dependent density functional theory excitation energies seems to provide a promising route to the geometry optimization of excited states for larger molecules. Here, the application of the standard TDDFT/B3LYP has shown its limits but we are sure that the exploration of different functionals, especially the most recent ones accounting for long-range corrections [36–39] and thus most suited to properly describe CT excited states, would lead to better results.

In any case, both TT and STD theories may be now translated into efficient computational approaches which can be easily applied also to larger molecular systems and they can take into account solvent effects. In particular, QM continuum solvation methods such as PCM seem to represent a promising way to couple these theories with an accurate and efficient solvation model. Clearly, further extensions with respect to what presented here are not only possible but also already initiated. The inclusion of solvent effects into the shape of the RR band and not only on its position and intensity, is one of these extensions. In this case, a real time-dependent picture of the solvent polarization should be used; this type of approach has been already presented for TD stokes shifts and other relaxation processes [10,40,41] and it should not be difficult to reformulate it for the present problem. Another possible research line is the extension of PCM to the new method which has been developed by Schatz et al. [42] to describe the Raman scattering cross section. This method is still based on a short-time approximation and it makes it possible to calculate both normal Raman scattering and resonance Raman scattering intensities from the geometrical derivatives of the frequency-dependent polarizability (real or complex). As said above, PCM has been already extended to treat NRS by including solvent effects in the real part of the frequency-dependent polarizability (and its derivatives) [24] and thus an extension to the complex part is surely feasible. This should thus permit to treat RRS of solvated systems in a more general framework without requiring any of the strong approximations used in both TT and STD, such as assuming only one excited state to determine the RR spectrum.

**Acknowledgment** Financial support by the Italian MIUR (Ministero dell'Istruzione, Università e Ricerca), PRIN 2005, and by Gaussian Inc. is here acknowledged.

## References

1. Myers AB (1996) Chem Rev 96:911
2. Miertus S, Scrocco E, Tomasi J (1981) Chem Phys 55:117
3. Cammi R, Tomasi J (1995) Comput Chem 16:1449
4. Cancès E, Mennucci B, Tomasi J (1997) J Chem Phys 107:3032
5. Mennucci B, Cancès E, Tomasi J (1997) J Phys Chem B 101:10506
6. Tomasi J, Mennucci B, Cammi R (2005) Chem Rev 105:2999
7. Mennucci B (2006) Theor Chem Acc 116:31
8. Cammi R, Corni S, Mennucci B, Tomasi J (2005) J Chem Phys 122:104513
9. Corni S, Cammi R, Mennucci B, Tomasi J (2005) J Chem Phys 123:134512
10. Caricato M, Mennucci B, Tomasi J, Ingrosso F, Cammi R, Corni S, Scalmani G (2006) J Chem Phys 124:124520
11. Cammi R, Mennucci B, Tomasi J. (2000) J Phys Chem A 104:5631
12. Scalmani G, Frisch M, Mennucci B, Tomasi J, Cammi R, Barone V (2006) J Chem Phys 124:094107
13. Peticolas WL, Rush T III (1995) J Comput Chem 16:1261
14. Lee S-Y, Heller EJ (1979) J Chem Phys 71:4777
15. Heller EJ, Sundberg RL, Tannor D (1982) J Phys Chem 86:1822
16. Kramers HA, Heisenberg W (1925) Z Phys 31:681
17. Dirac PAM (1927) Proc R Soc Lond Ser A 114:710
18. Blazej DC, Peticolas WL (1980) J Chem Phys 72:3134
19. Chan CK Page JBJ (1983) Chem Phys 79:5234
20. Wilson EB, Decius JC, Cross PC (1955) Molecular vibrations. McGraw-Hill:New York
21. Li B, Johnson AE, Mukamel S, Myers AB (1994) J Am Chem Soc 116:11039
22. Neugebauer J, Hess BA (2004) J Chem Phys, 120:11564
23. Cammi R, Cappelli C, Corni S, Tomasi J (2000) J Phys Chem A 104:9874
24. Cappelli C, Corni S, Tomasi J (2001) J Chem Phys 115:5531
25. Tomasi J, Cammi R, Mennucci B, Cappelli C, Corni S (2002) Phys Chem Chem Phys 4:5697

26. Aguilar MA, Olivares Del Valle FJ, Tomasi J (1993) J Chem Phys 98:7375
27. Cammi R, Tomasi J (1995) Int J Quant Chem Symp 29:465
28. Mennucci B, Cammi R, Tomasi J (1998) J Chem Phys 109:2798
29. Moran AM, Egolf DS, Blanchard-Desce M, Myers Kelley A (2002) J Chem Phys 116:2542
30. Myers Kelley A. (2005) Int J Quantum Chem 104:602
31. Moran AM, Myers Kelley A, Tretiak S (2003) Chem Phys Lett 367:293
32. Frisch MJ et al (2004) GAUSSIAN, Development Version, Revision D.02, Gaussian, Inc., Wallingford, CT
33. Tozer DJ, Amos RD, Handy NC, Roos BO, Serrano-Andres L (1999) Mol Phys 97:859
34. Dreuw A, Weisman JL, Head-Gordon M (2003) J Chem Phys 119:2943
35. Bernasconi L, Sprik M, Hutter J (2003) J Chem Phys 119:12417
36. Ikura H, Tsuneda T, Yanai T, Hirao K (2001) J Chem Phys 115:3540
37. Yanai T, Tew DP, Handy NC (2004) Chem Phys Lett 393:51
38. Tawada Y, Tsuneda T, Yanagisawa S, Yanai T, Hirao K (2004) J Chem Phys 120:8425
39. Chiba M, Tsuneda T, Hirao K (2006) J Chem Phys 124:144106
40. Ingrosso F, Mennucci B, Tomasi J (2003) J Mol Liq 108:21
41. Caricato M, Ingrosso F, Mennucci B, Tomasi J (2005) J Chem Phys 122:154501
42. Jensen L, Zhao LL, Autschbach J, Schatz GC (2005) J Chem Phys 123:174110